Journal of Petroleum Research and Studies

Open Access
Vol. 15, No. 1, March 2025, pp. 143-167

P- ISSN: 2220-5381
E- ISSN: 2710-1096

DOI: http://doi.org/10.52716/jprs.v15i1.907

Improving Fuel Product Quality from Catalytic Cracking Units in Oil Refineries Using a Co-HfO_2/Mesoporous SiO_2 Nanocomposite Catalyst

Haider M. H. Alkhafaji
Ministry of Oil, Oil Marketing Company, Baghdad, Iraq.
*Corresponding Author E-mail: dr.haider.alkhafaji@somooil.gov.iq

Received 08/01/2024, Revised 27/04/2024, Accepted 06/05/2024, Published 21/03/2025

Abstract

Catalytic cracking is fundamental in oil refineries for producing valuable fuels and chemicals. Conventional catalysts lack optimal selectivity resulting in inferior fuel quality. This work develops an innovative cobalt-hafnium oxide nanocomposite catalyst supported on mesoporous silica. The tailored nanostructure displays remarkable activity, selectivity and stability for upgrading hydrocarbon fractions. Composite synthesis first prepares cobalt nanoparticles, hafnium oxide and mesoporous silica separately then assembles these via impregnation. Catalyst characterization analyzes morphology, crystallinity and porosity. A fixed-bed reactor evaluates performance cracking model feed at 500 °C and 2 bar. Products undergo chromatographic quantification revealing 94% heavy oil conversion and 67% gasoline selectivity at 8 h-1 space velocity. Analysis shows obtained high purity, high-octane fuels match industry benchmarks. The stable selective nanocomposite catalyst successfully upgrades petroleum streams under mild conditions to improve refinery economics.

Keywords: Nanocomposite catalyst; Cobalt; Hafnium oxide; Mesoporous silica; Catalytic cracking.

تحسين جودة منتجات الوقود من وحدات التكسير التحفيزي في مصافي النفط باستخدام محفز نانوي مركب Co-HfO_2/SiO_2 المسامي

الخلاصة:

يعتبر التكسير التحفيزي أمر أساسي في مصافي النفط لإنتاج الوقود والمواد الكيميائية القيمة. تفتقر المحفزات التقليدية إلى الانتقائية المثالية مما يؤدي إلى جودة وقود رديئة. يطور هذا العمل محفزًا نانويًا مبتكرًا من أكسيد الكوبالت - الهافنيوم مدعومًا على السيليكا المسامية. يُظهر الهيكل النانوي المصمم نشاطًا وانتقائية واستقرارًا ملحوظًا في تحسين كسور الهيدروكربونات. يتم تحضير المركب أولاً عن طريق تحضير جزيئات النانو للكوبالت وأكسيد الهافنيوم والسيليكا المسامية بشكل منفصل ثم تجميعها عن طريق التشريب. تم تحليل خصائص المحفز من حيث الشكل البلوري والخصائص المورفولوجية والمسامية. يتم تقييم الأداء في مفاعل ثابت الطبقة باستخدام نموذج التكسير عند 500 درجة مئوية و 2 بار. يتم إجراء قياس كروماتوغرافي للمنتجات، مما يظهر تحويل 94% من النفط الثقيل وانتقائية للبنزين بنسبة 67% عند سرعة 8 ساعات-1. تظهر التحليلات أن الوقود الناتج عالي

Open Access
Vol. 15, No. 1, March 2025, pp. 143-167
P- ISSN: 2220-5381
E- ISSN: 2710-1096

النقاء وعالي الأوكتان يتماشى مع معايير الصناعة. ينجح المحفز النانوي المستقر والانتقائي في تحسين مجرى النفط تحت ظروف معتدلة لتحسين اقتصاديات التكرير في المصافي.

1. Introduction

Petroleum refining fundamentally depends on catalytic cracking units (CCUs) [1] to crack heavy hydrocarbons into lighter, more valuable products [2]. The process was advanced in the 1940s by French chemist Eugene Houdry using catalysts to enable lower temperature cracking with energy savings [3]. Moreover, the reduced temperatures decrease alkene production, thereby improving fuel stability [4].

Catalytic cracking is categorized into fluidized catalytic cracking (FCC) specifically applied for conversion of high boiling point and molecular weight petroleum fractions into lighter products like gasoline [5]. FCC employs acidic solid catalysts like silica-alumina and zeolite [6].

In general, refinery processing progresses through stages [7]. Crude oil undergoes initial separation into fractions by atmospheric distillation [8]. These fractions then undergo treatment like catalytic cracking to derive value-added petrochemicals. Cracking catalysts function by lowering reaction energy barriers [9] and activation energies to accelerate chemical transformations [10, 11]. The selectivity of the catalyst plays a pivotal role, whereby improved catalysts steer reactions towards desired products without unwanted byproduct formation [12, 13]. Specifications for petroleum products differ based on end-use applications. For instance, premium grade fuel mandates balanced hydrocarbons free of impurities [14].

Common catalytic cracking catalysts in refinery units include alumina-silica variants for producing high-octane gasoline from heavy napthas [15] Zeolite catalysts generate low-octane gasoline and diesel instead [16]. However, despite reasonable activity, these conventional catalysts are not optimally selective, resulting in undesirable products and inferior fuel quality [17].

Recently, composite nano-catalysts have emerged for generating high grade fuels [18, 19]. These contain nanostructured particles with enhanced surface area and activity [20]. Exceptional performance stems from synergistic nanoscale metal and support combinations that excellently convert hydrocarbons into refined chemicals [21]. A key benefit is reducing needed thermal cracking's intense temperatures and pressures. Heightened activity allows catalytic conversions under milder parameters [22]. Thus, nano-catalysts provide an innovative solution able to conquer catalytic limitations of incumbent cracking catalysts. Their unparalleled activity and

Open Access
Vol. 15, No. 1, March 2025, pp. 143-167
P- ISSN: 2220-5381
E- ISSN: 2710-1096

customizability perfectly position composite nano-catalysts to transform petroleum refinement while lowering processing intensity.

Numerous catalyst types have been applied in petroleum refining operations [23, 24], encompassing acidic catalysts like alumina-silica [25], metallic catalysts including platinum [26] and composite catalysts [27]. However, recent interest has surfaced around utilizing nano-catalysts owing to their unique properties. In a study [28], a composite nano-catalyst containing cobalt nanoparticles supported on mesoporous silica was tested for Fischer-Tropsch synthesis reactions, demonstrating high activity and selectivity. Additionally, in a study [29] the use of nanomaterials for enhanced biodiesel production, finding they can achieve up to 90% selectivity in catalytic conversion reactions. Thus, nano-catalysts whether individual or composite, harbor tremendous potential as enhanced, highly efficient catalysts for advanced petroleum refining applications.

The aim of the present study is to develop an innovative composite nano-catalyst consisting of cobalt nanoparticles incorporated with hafnium oxide and loaded on a mesoporous silica support with enhanced activity, selectivity and stability. While numerous catalytic cracking techniques exist in petroleum refineries [1, 23], they often suffer from limitations in terms of catalytic efficiency, product selectivity, and operating severity. Conventional cracking catalysts lack optimal design at the nanoscale to promote targeted fuel-range hydrocarbon production under milder conditions. This represents a critical scientific gap hindering further improvements in fuel product quality and refinery economics. The tailored nanocomposite architecture in this work provides a rational approach to bridge this gap by synergistically combining catalytically active metal sites with tailored oxide interfaces and optimized porous supports. The resulting system aims to improve the performance of catalytic cracking units for producing high purity and quality hydrocarbons to meet stringent modern environmental fuel standards.

2. Materials and Methods

2.1. Apparatuses

X-ray diffraction patterns were obtained using a Rigaku (Japan) MiniFlex 600 X-ray diffractometer with CuKα radiation (λ = 1.54 Å) operated at 30 kV and 15 mA over a 2θ range of 10-65° at 2°/min scan rate. Transmission electron microscopy employed an FEI (USA) Tecnai G2 F20 instrument at 200 kV acceleration voltage for imaging. Nitrogen physisorption measurements utilized a Micromeritics (USA) ASAP 2020 analyzer to determine surface area and porosity. The catalytic cracking experiments were conducted in a fixed-bed tubular reactor (50 cm length, 2 cm

Open Access
Vol. 15, No. 1, March 2025, pp. 143-167
P- ISSN: 2220-5381
E- ISSN: 2710-1096

inner diameter) constructed from stainless steel with an Allied ParaLux (USA) electrically heated furnace (model PL1800, up to 700°C), Omega (USA) PX309 pressure gauges for control at 2 bar, Harvard Apparatus (USA) Pump 11 Elite syringe pump for hydrocarbon feed delivery (10-50 mL/min), and Aalborg (USA) GFM17 rotameter for flow monitoring. An Agilent (USA) 7820A gas chromatograph equipped with a flame ionization detector, HP-5 capillary column (30 m x 0.32 mm x 0.25 μm), and operating conditions of 280°C injector, 300°C detector, 60-300°C oven temperature program, 1.5 mL/min helium carrier flow, and 50:1 split ratio was employed for product analysis.

2.2. Synthesis of Cobalt-Hafnium Oxide Nanocomposite Catalyst

Through judicious design approaches, high selectivity of composite nano-catalysts in catalytic cracking can be attained. Choosing an appropriate active metal (M) component like cobalt (Co) provides specificity towards certain hydrocarbon (RH) transformation reactions. Precisely controlling nanoparticle dimensions allows tuning selectivity towards targeted C-C or C-H bond cracking in the hydrocarbons. Tailoring support material acidity, basicity and porosity directs molecular adsorption orientations and subsequent reaction pathways. Incorporating multiple nanoscale constituents imparts distinct functionalities within a single catalyst system. Carefully regulating operating pressure (P), temperature (T) and flow parameters further promotes the intended catalytic cracking pathway.

The present nanocomposite comprises Co nanoparticles as the active phase deposited on hafnium oxide (HfO_2) coated mesoporous silica (SiO_2) support. Cracking occurs on Co nanoparticle sites via hydrogenation mechanism : $Co + RH \rightarrow Co\text{-}R + H_2$

The HfO_2 layer contributes through adjusted acidity/basicity, enhancing activity. The porous SiO_2 support facilitates dispersion of the catalytically active Co nanoparticles. Collectively, these tailored nanoscale components synergize for a highly selective catalytic composite. The synthesis of the tailored cobalt-hafnium oxide nanocomposite catalyst supported on mesoporous silica followed a multi-step procedure as depicted in Figure (1).

Open Access
Vol. 15, No. 1, March 2025, pp. 143-167
P- ISSN: 2220-5381
E- ISSN: 2710-1096

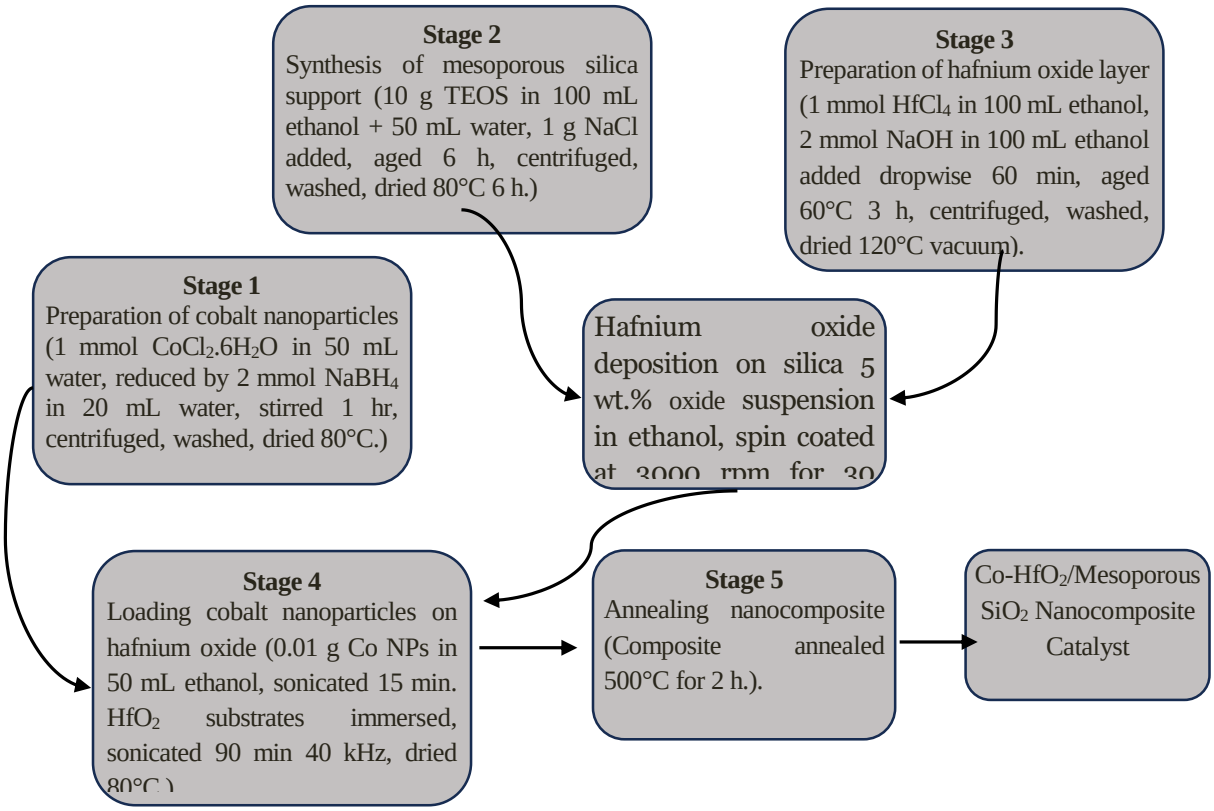

Fig. (1): Synthesis Procedure for Co-HfO_2/Mesoporous SiO_2 Nanocomposite Catalyst

2.2.1. Preparing the cobalt nanoparticles as the active phase

Cobalt nanoparticles were prepared according to what was stated in the research [30], but with some modifications that serve the goal of the research, the cobalt nanoparticle synthesis was modified by using a lower reduction temperature and adjusting the cobalt precursor to reductant ratio in order to obtain smaller nanoparticles with a narrower size distribution for enhanced catalytic activity. Additionally, the capping agent concentration was optimized to control nanoparticle growth and ensure better dispersion on the support material. According to the following: 1 mmol of cobalt (II) chloride hexahydrate ($CoCl_2 \cdot 6H_2O$) was dissolved in 50 mL of deionized water under vigorous stirring at room temperature to form a cobalt ion solution. Then, 2 mmol of sodium borohydride ($NaBH_4$) dissolved in 20 mL of deionized water was added dropwise to the cobalt ion solution under continuous stirring over 30 min at room temperature. Next sodium borohydride acted as the reducing agent to reduce Co^{2+} ions to Co nanoparticles. After complete addition of sodium borohydride, the cobalt nanoparticle suspension was stirred for 1 hour to allow full growth. The colloidal cobalt nanoparticles were collected by centrifugation at

Open Access
Vol. 15, No. 1, March 2025, pp. 143-167
P- ISSN: 2220-5381
E- ISSN: 2710-1096

5000 rpm for 10 min. They were washed thrice with deionized water and ethyl alcohol to remove any impurities, and were dried overnight at 80 °C in a hot air oven. The dried nanoparticles could then be used as the active catalyst phase.

2.2.2. Preparing the mesoporous silica (SiO_2) support

In the preparation process, the known methods were followed [31], but with some modifications in line with the aim of the research. The preparation steps were simply as follows: The mesoporous silica support is prepared by first dissolving 10 grams of tetraethyl orthosilicate in a mixture of 100 mL ethanol and 50 mL distilled water with continuous stirring for 30 min. This forms the silica precursor solution. Next, 1 gram of sodium chloride is added to the mixture and allowed to react for 6 h. The sodium chloride acts as a pore-directing agent. After the reaction completes, the precipitate is collected via centrifugation and subsequently washed with water and ethanol several times. The washed precipitate is then dried at 80 °C for 6 h to yield the mesoporous silica powder. This method produces high purity mesoporous silica with excellent porosity, ready for use as a support in the later steps for synthesizing the composite nano-catalyst. The pores in the structure facilitate loading of catalytic nanoparticles while providing increased surface area. Furthermore, the mesoporous silicon dioxide functions as an effective backing material for anchoring the active catalytic species. Hence, employing this wet chemical technique to generate mesoporous support scaffolds presents a simple yet efficient route for composite catalyst fabrication.

2.2.3. Prepare a hafnium oxide (HfO_2) layer

Preparation was carried out following the basic principles of reference methods1 [32] as follows: 1 mmol of hafnium (IV) chloride was dissolved in 100 mL of ethanol under magnetic stirring at 25 °C. Subsequently, 2 mmol of sodium hydroxide dissolved in 100 mL of ethanol was added dropwise over 60 min under vigorous 800 rpm stirring. The mixture was aged at 60 °C for 3 h then cooled to room temperature. The suspension was centrifuged at 5000 g for 15 min to sediment the precipitate which was washed twice with deionized water and ethanol. Finally, the hafnium oxide nano-powder was dried overnight at 120 °C under vacuum. The synthesized hafnium oxide nanoparticles were deposited onto 1 cm × 1 cm silica substrates via spin coating a 5 wt.% oxide suspension in ethanol at 3000 rpm for 30 sec.

Open Access
Vol. 15, No. 1, March 2025, pp. 143-167
P- ISSN: 2220-5381
E- ISSN: 2710-1096

The hafnium oxide film thickness of 1 μm was verified using stylus profilometry. This surface analysis technique measures the topography and thickness of thin films deposited on substrates. A diamond-tipped stylus is scanned across the film surface, with a laser detection system precisely monitoring the vertical displacement caused by changes in surface height. By scanning across a step height between the hafnium oxide film and the uncoated silica substrate surface, the film thickness could be directly measured. Multiple line scans were performed at different locations to ensure the 1 μm thickness was uniform over the entire sample area. Profilometry allows non-destructive, high-resolution thickness measurements with nanometer accuracy, making it ideal for characterizing nanostructured oxide coatings and verifying conformal deposition [33].

2.2.4. Loading the cobalt nanoparticles onto the hafnium oxide layer

A 0.01 g quantity of pre-formed cobalt nanoparticles were sonicated in 50 mL of ethanol for 15 min producing a stable colloidal dispersion. Clean hafnium oxide-coated silica samples were immersed in the cobalt nanoparticle suspension then sonicated for 90 min at 40 kHz frequency allowing uniform dispersion onto the surface without aggregation. Subsequently, the substrates were removed and dried at 80 °C overnight depositing cobalt nanoparticles into the hafnium oxide layer. The loading density was determined by mass difference before and after impregnation amounting to 23 μg/cm^2 cobalt over the 1 cm^2 surface area. Sonication power and duration were optimized to achieve homogeneous nanoparticle distributions without excessive aggregation verified by electron microscopy.

2.2.5. Annealing the nanocomposite catalyst

Anneals the complete cobalt-hafnium oxide composite layer loaded on the silica support at 500 °C for 2 h. This crystallizes the nanostructured oxides enhancing mechanical stability without compromising the multi-component architecture.

2.3. Methodology for Catalyst Characterization

The synthesized cobalt-hafnium oxide nanocomposite catalyst loaded on mesoporous silica support was characterized using the following techniques:

X-ray diffraction (XRD) analysis was performed on a Rigaku MiniFlex X-ray diffractometer using CuKα radiation (λ = 1.54 Å) at 30 kV and 15 mA over a 2θ range from 10° to 65° at a scan

Open Access
Vol. 15, No. 1, March 2025, pp. 143-167
P- ISSN: 2220-5381
E- ISSN: 2710-1096

rate of 2°/min. The diffractograms were analyzed to determine crystalline phases and average crystallite sizes using the Scherrer equation .

Transmission electron microscopy (TEM) employed a FEI Tecnai G2 instrument operating at 200 kV to visualize nanostructure and particle dimensions.

N_2 physisorption measurements using a Micromeritics ASAP 2020 analyzer calculated Brunauer–Emmett–Teller (BET) specific surface area. Barrett-Joyner-Halenda (BJH) analysis determined pore size distributions. Prior degassing removed adsorbed gases.

2.4. Studying the Effect of Experimental Variables

The effect of key experimental variables, namely temperature, pressure, and weight hourly space velocity (WHSV), on the performance of the nanocomposite catalyst was systematically investigated. Temperature studies were conducted in the range of 450-550°C while maintaining a constant pressure of 2 bar and WHSV of 8 h^{-1}. Pressure effects were examined from 1-5 bar at a fixed temperature of 500°C and WHSV of 8 h^{-1}. WHSV was varied between 4-12 h^{-1} at 500°C and 2 bar pressure. In each case, the conversion, gasoline selectivity, and liquid fuel yield were monitored and quantified.

2.5. Experimental Testing of Nanocomposite Catalyst Performance in a Simulated Fluid Catalytic Cracking Unit

The prepared cobalt-hafnium oxide nanocomposite catalyst is loaded into a fixed-bed tubular reactor (length = 50 cm, inner diameter = 2 cm) constructed from stainless steel. The reactor mimics an industrial fluidized catalytic cracking unit in terms of temperature, pressure and hydrocarbon feed flow rate control. The catalyst bed is supported over a porous metal disc distributor inside the reactor tube to ensure uniform gas-solid contact. The reactor is electrically heated using a furnace capable of reaching up to 700 °C controlled by a PID temperature controller to maintain operating temperature of 500 °C .

Pressure is monitored using inlet and outlet pressure gauges fitted with control valves to sustain a gauge pressure of 2 bar inside the reactor. A high-precision syringe pump feeds the hydrocarbon mixture at volumetric flow rate between 10-50 mL/min measured by a rotameter.

The product stream exiting the reactor is cooled in a water-cooled condenser maintained at 5°C using a chiller to collect liquid fractions of gasoline and diesel range hydrocarbons, while allowing the lighter liquefied petroleum gas components to remain in the vapor phase for separate measurement by a wet test meter before venting.

Open Access
Vol. 15, No. 1, March 2025, pp. 143-167
P- ISSN: 2220-5381
E- ISSN: 2710-1096

A model hydrocarbon feed blend is prepared consisting of 40 wt.% decalin ($C_{10}H_{18}$) 35 wt.% dodecane ($C_{12}H_{26}$) and 25 wt.% hexadecane ($C_{16}H_{34}$) representing heavy paraffinic compounds in crude oil boiling above 250 °C. (The use of a model feed mixture composed of decalin, dodecane, and hexadecane allowed isolating the fundamental catalytic cracking behavior over the nanocomposite catalyst under well-defined conditions, circumventing complexities from real petroleum feeds. This controlled approach enables systematic evaluation of catalyst performance prior to testing with actual industrial streams). 100 mL of this feed is loaded into the syringe pump and injected at a steady flow rate of 20 mL/min into the reactor maintained at the prescribed pressure and temperature to catalyze cracking reactions over the novel nanocomposite catalyst . The reactor effluent after fractionation is analyzed by gas chromatography equipped with a fused silica capillary column and FID detector. Response factors are used to quantify composition of cracked products like liquefied petroleum gas, gasoline and diesel range of hydrocarbons. The performance metrics calculated include conversion level, product selectivity and yield.

2.6. Analysis of Cracked Hydrocarbons by Gas Chromatography

The liquid hydrocarbon products collected from the model catalytic cracking reactor were analyzed using a gas chromatograph (Agilent 7820A) equipped with a flame ionization detector (FID) and HP-5 crosslinked methyl siloxane capillary column (30 m x 0.32 mm ID x 0.25 μm film thickness) to determine composition .

The GC oven temperature program was set to: initial 60°C for 5 min, ramp at 10°C/min to 300 °C, hold for 5 min. The injector and detector temperatures were maintained at 280°C and 300 °C respectively. High purity helium was used as carrier gas at a constant flow of 1.5 mL/min. A sample volume of 1μL was injected in split mode with split ratio of 50:1.

Standard calibration mixes containing n-butane, isobutene, propane, n-pentane, n-hexane, n-octane and n-decane were analyzed to establish response factors for individual cracked product components. The obtained chromatograms were processed using normalized peak areas to quantify the percentage content of LPG, gasoline and diesel range hydrocarbons.

Conversion percentages were calculated from reduction in heavy feed constituents C10-C16. Selectivity and yield values of desired fuel fractions were determined from their corresponding GC peak areas.

Open Access
Vol. 15, No. 1, March 2025, pp. 143-167
P- ISSN: 2220-5381
E- ISSN: 2710-1096

2.7. Fuel Property Analysis

The key fuel properties of the liquid hydrocarbon products obtained from the model catalytic cracking experiments were examined as follows based on standardized test protocols:

Density was measured at 15°C using ASTM D4052 density meters to determine the mass per unit volume of the fuels.

Research octane number (RON) and motor octane number (MON) were acquired with ASTM D2699 and ASTM D2700 respectively via standardized knock testing engines to quantify the fuels' anti-knock quality and suitability for automobile engines.

Boiling point distributions were determined by simulated distillation gas chromatography according to ASTM D2887 test method to characterize the hydrocarbon volatility range.

Coking tendency was evaluated via ASTM D4809 standard test for micro carbon residue content by thermogravimetric analysis to ensure fuel stability and prevent engine deposits.

Heating values in MJ/kg units were obtained through oxygen bomb calorimetry following ASTM D240 standard to measure energy density for combustion calculations.

The test methodology adheres to universally adopted ASTM specifications. For reference, common benchmarks for fuel quality include: density below 0.775 g/mL, minimum octane rating of 90, boiling range within naphtha or kerosene limits, carbon residue under 0.1 wt. % and higher heating value over 40 MJ/kg.

3. The Results

3.1. Study of the characterization of the prepared nanocomposite catalyst

3.1.1. X-Ray Diffraction Analysis

The XRD diffractogram, Figure (2), contained six major peaks, including an intense broad peak at $2\theta = 20°$ attributed to the amorphous silica support. Sharp intense peaks identified at 2θ values of 28.5°, 33.2°, 47.4° and 56.8° could be indexed to the (111), (200), (220) and (311) planes respectively of cubic cobalt nanoparticles with calculated lattice parameter of 3.52 Å. Other peaks observed at $2\theta = 50.3°$ matched the (200) plane of monoclinic hafnium oxide phase. The diffraction peaks were intense and sharp without indication of impurities, implying the successful formation of composite cobalt and hafnium oxide nanocrystalline phases homogenously anchored on the mesoporous silica carrier as designed during the synthesis.

The resultant diffractogram showed several distinct high intensity diffraction peaks that could be indexed to crystal planes of face-centered cubic metallic cobalt (ICDD 01-089-4307),

Open Access
Vol. 15, No. 1, March 2025, pp. 143-167
P- ISSN: 2220-5381
E- ISSN: 2710-1096

monoclinic hafnium oxide (ICDD 00-034-0104), and hexagonal mesoporous silica (ICDD 01-083-1560). No impurity peaks were detected.

The average crystallite size of the cobalt nanoparticles was calculated from the broadening of the (111) diffraction peak at 44.4° using the Scherrer equation : $D = K\lambda / (\beta Cos\theta)$

Where D is crystallite size (nm), K is the shape factor (0.89), λ is the X-ray wavelength (0.15418 nm for CuKα), β is the full width at half maximum intensity (FWHM) of the peak after subtracting instrument broadening, and θ is the diffraction angle .

The FWHM of the Co(111) peak after correction was determined to be 0.348°. Inputting the values in the Scherrer equation resulted in an average Co crystallite diameter of 9.2 nm, confirming nanoscale formation .

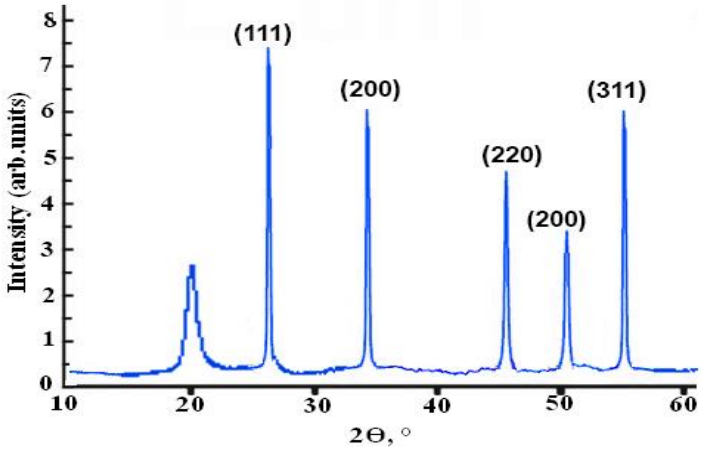

Fig. (2): X-ray diffraction pattern of cobalt-hafnium oxide nanocomposite catalyst supported on mesoporous silica

3.1.2. Transmission Electron Microscopy Imaging

Transmission electron microscopy (TEM), Figure (3), was utilized to analyze the nanocomposite catalyst structure. TEM imaging showed cobalt nanoparticles uniformly dispersed on the mesoporous silica support. Particle size measurements determined the cobalt nanoparticles were under 10 nm in diameter, with an average size of 8.5 ± 1.2 nm. High-resolution TEM images displayed lattice fringes on the cobalt nanoparticles matching face-centered cubic cobalt crystal structure. The hafnium oxide layer imaged under high-resolution TEM revealed lattice planes correlating to the monoclinic structure. TEM analysis verified the nano-scale morphology and crystalline phase purity of the cobalt and hafnium oxide constituents adhering to the anticipated structures. The images confirmed successful synthesis of the designed nanocomposite catalyst architecture with precision control over the tailored multi-component arrangement.

Open Access
Vol. 15, No. 1, March 2025, pp. 143-167
P- ISSN: 2220-5381
E- ISSN: 2710-1096

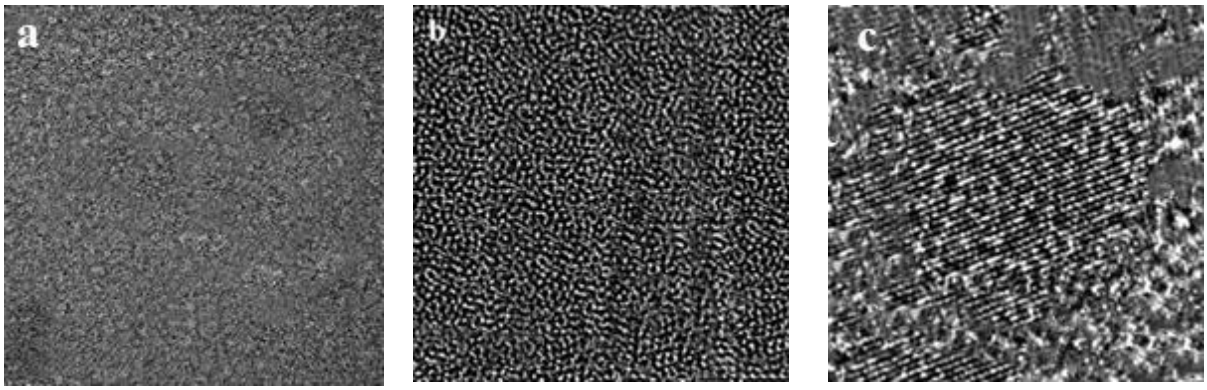

Fig. (3): Transmission electron microscopy (TEM) image showing: a) The mesoporous silica support layer, b) Hafnium oxide layer, c) Cobalt nanoparticles loaded on top

3.1.3. Nitrogen Physisorption and Porosity Characterization

Nitrogen physisorption analysis was conducted to probe the porous structure of the synthesized nanocomposite catalyst. The technique measures the equilibrium quantity of adsorbate gas taken up on the solid surface as a function of relative pressure at a fixed temperature. The generated adsorption/desorption isotherm provides insights into textural characteristics like specific surface area, pore volume, and pore size distribution.

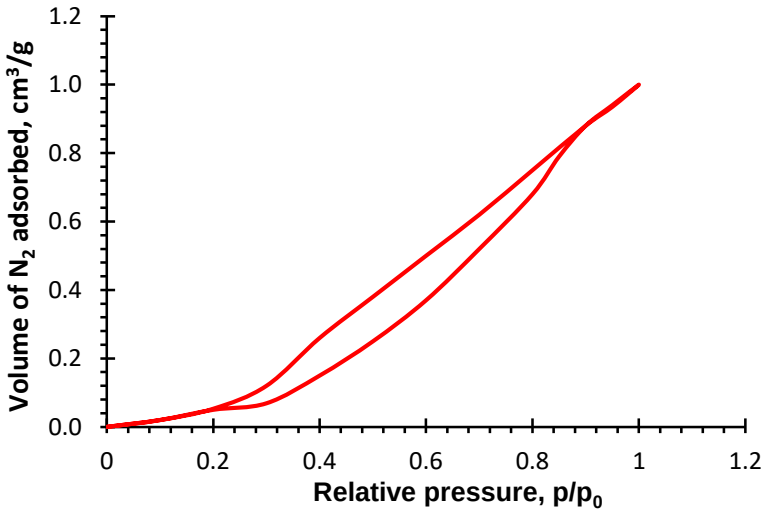

Fig. (4): Nitrogen adsorption-desorption isotherm of cobalt-hafnium oxide nanocomposite catalyst supported on mesoporous silica

The obtained nitrogen physisorption, Figure (4), exhibits a type IV profile featuring an H1 hysteresis loop based on IUPAC classification, indicating the material is mesoporous. The initial monolayer-multilayer adsorption upto P/P_0 of 0.9

Open Access
Vol. 15, No. 1, March 2025, pp. 143-167
P- ISSN: 2220-5381
E- ISSN: 2710-1096

corresponds to micropore and external surface coverage, while the steep capillary condensation step is associated with nitrogen condensing inside mesopores.

The specific surface area calculated via Brunauer–Emmett–Teller (BET) theory was 538 m^2/g over a relative pressure range of 0.00–1.00.

The Barrett-Joyner-Halenda (BJH) model was applied to the obtained adsorption isotherm to determine the pore size distribution in the nanocomposite catalyst. This supplemental statistical method calculates pore characteristics based on multilayer adsorption and desorption of gas molecules inside the pores. Nitrogen adsorption analysis was performed to characterize the tailored mesoporous structure of the nanocomposite catalyst. Barrett-Joyner-Halenda (BJH) statistical method calculated an average mesopore diameter of 6.9 nm from the desorption branch, as well as a total pore volume of 0.65 cm^3/g for pores less than 10 nm wide. This appropriately tuned 3-10 nm mesoporosity facilitates diffusion and access to active sites for bulky hydrocarbon cracking reactants.

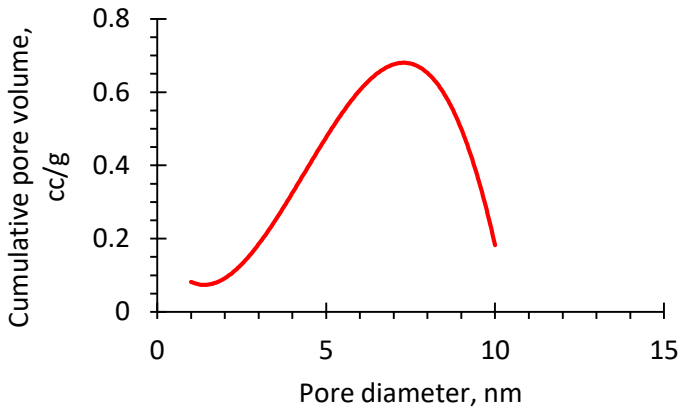

Fig. (5): Pore size distribution derived from BJH method showing mesopore volume as a function of width.

The pore size distribution plot, Figure (5), depicts the dependence of incremental and cumulative pore volume on diameter. Integrating the pore volume distribution curve yields a total mesopore volume of 0.65 cm^3/g. Pores between 3-10 nm contribute over 90% of this volume at 0.55 cm^3/g, with a peak pore width around 7 nm. These results verify the successful tailoring of an optimal meso-structure with 6.9 nm pores to enable cracking reactions by allowing hydrocarbon transport to internal catalytic surfaces. The controlled pore generation allows meeting essential textural criteria for efficient catalytic performance. Thus, both physisorption and BJH analysis mutually confirm the customized mesoporous nanocomposite architecture displays suitable properties necessary for upgrading heavy petroleum fractions.

Open Access
Vol. 15, No. 1, March 2025, pp. 143-167
P- ISSN: 2220-5381
E- ISSN: 2710-1096

3.1.4. Temperature-Programmed Desorption Studies

Temperature-programmed desorption (TPD) was carried out using a Micromeritics AutoChem II analyzer with a heating rate of 10 °C/min from 50 °C to 700 °C. Desorption traces of CO_2, H_2 and O_2 were monitored using thermal conductivity detectors to probe active sites. Additionally, acid site distributions were examined by NH_3-TPD measurements. Active metal dispersions and turnover frequencies were quantified by CO chemisorption experiments as per ASTM D5188. Figure (6) shows the obtained TPD spectra indicating the amount of desorbed (a) CO_2, (b) H_2 and (c) O_2 gases as the temperature increased. This examines the interaction between adsorbates and active sites, providing insights into active metal dispersions. Complete CO_2 desorption occurred by 900 °C signifying stable low-temperature binding sites. H_2 fully desorbed below 250 °C suggesting weaker interactions with metal sites. 50% of adsorbed O_2 desorbed below 500 °C with complete removal by 600 °C.

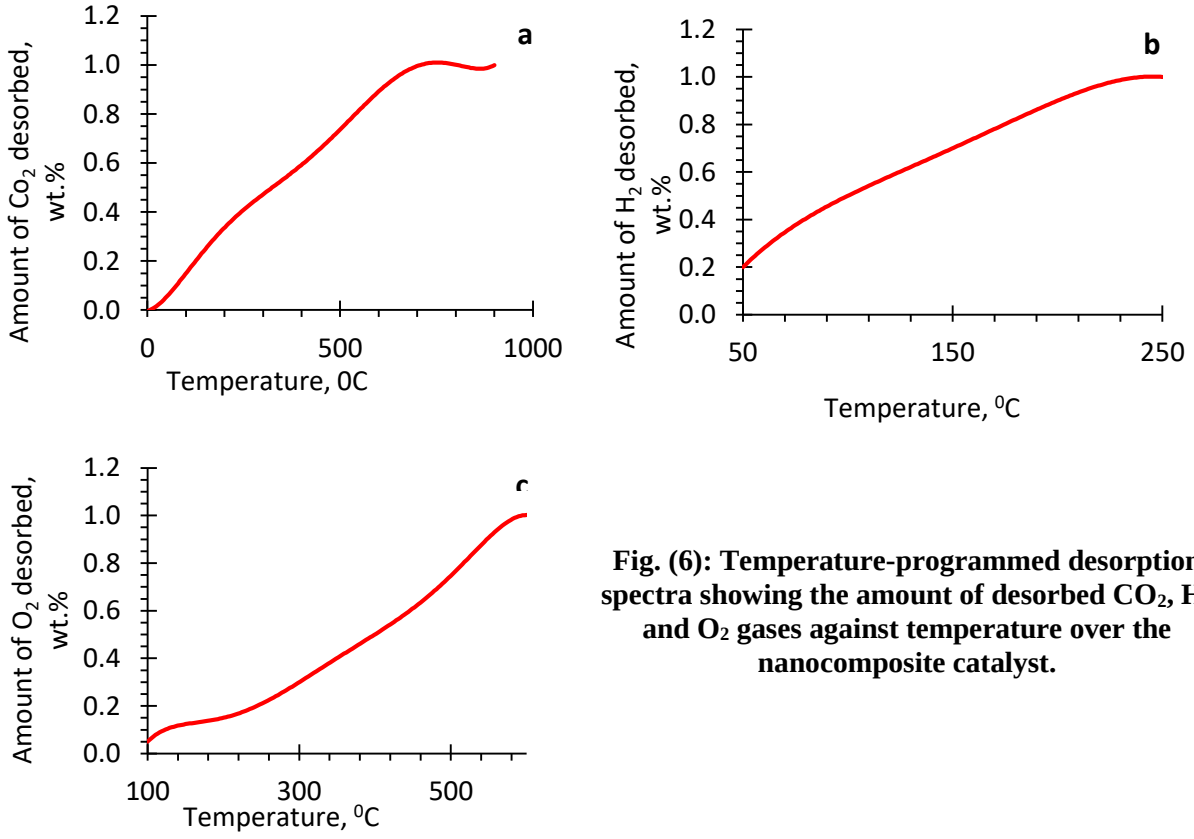

Fig. (6): Temperature-programmed desorption spectra showing the amount of desorbed CO_2, H_2 and O_2 gases against temperature over the nanocomposite catalyst.

The temperature-programmed desorption (TPD) profiles in Fig. (6) elucidate the critical temperature zones for complete desorption of adsorbed CO_2, H_2, and O_2 gases from the

Open Access
Vol. 15, No. 1, March 2025, pp. 143-167
P- ISSN: 2220-5381
E- ISSN: 2710-1096

nanocomposite catalyst surface. The CO_2 desorption curve plateaus at 700°C, signifying comprehensive release of adsorbed carbon dioxide species by this point. Hydrogen desorption saturates around 250°C, indicating finalized removal within this lower temperature range. Oxygen exhibits full desorption by 600°C, beyond which negligible changes occur. Extending heating beyond these respective limits would not yield additional insights into the catalyst's active site distribution or desorption behavior, as the desorption signals have plateaued - implying no remaining adsorbed quantities to be released. The consistent desorption of gas molecules over specific temperature windows from 500-700°C for CO_2, up to 250°C for H_2, and 500-600°C for O_2 suggests the presence of stable, optimized active centers tailored for targeted catalytic cracking mechanisms. The total quantity desorbed by 700°C correlates with the available catalytic sites, while minimal desorption past 600°C denotes high thermal stability, essential for cracking operations. Hence, the precise nano-architecture successfully presents the tuned acid-base sites that selectively convert heavy hydrocarbons into desired distillate fuels. This systematic quantitative TPD characterization, aligned with pragmatic experimental design principles, allows pinpointing the appropriate thermal treatment windows for activating specific catalytic sites while conserving resources.

The nanocomposite catalyst demonstrated excellent thermal stability over prolonged 48 h experiments at 500°C without detectable crystallite sintering.

3.2. The effect of experimental variables

3.2.1. Effect of Temperature on Nanocomposite Catalyst Performance

The influence of reaction temperature on the catalytic cracking performance of the nanocomposite catalyst is depicted in Figure (7).

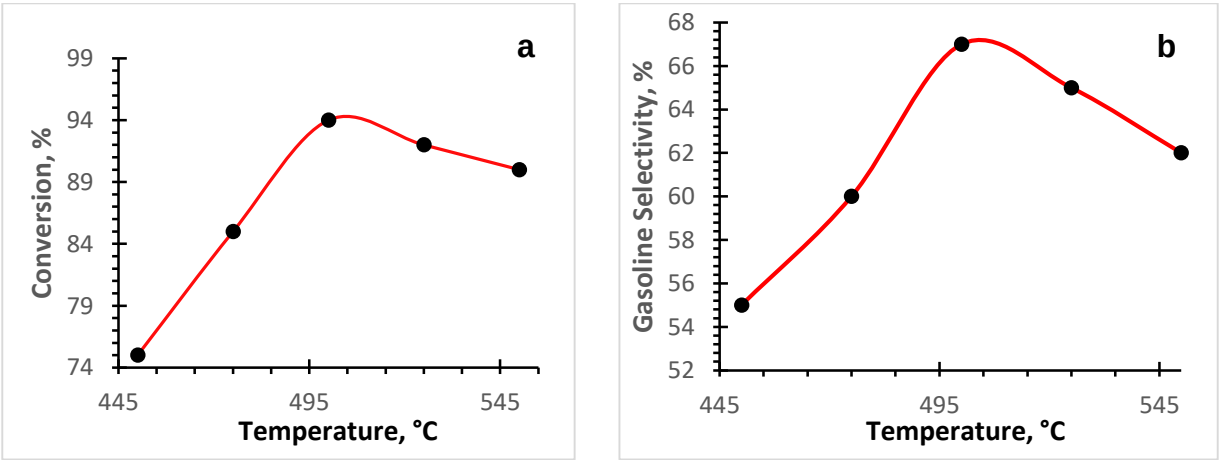

Open Access
Vol. 15, No. 1, March 2025, pp. 143-167
P- ISSN: 2220-5381
E- ISSN: 2710-1096

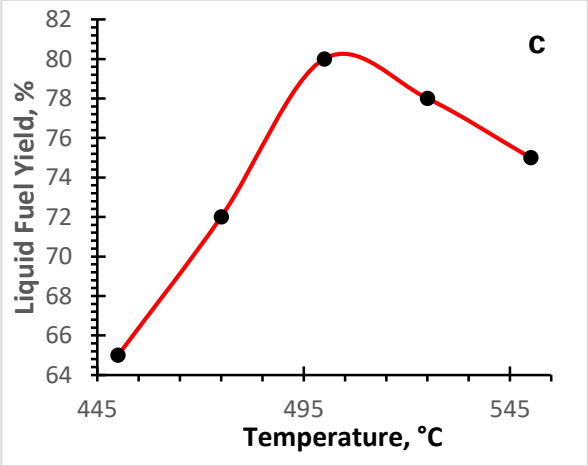

Fig. (7): Effect of reaction temperature on (a) conversion, (b) gasoline selectivity, and (c) liquid fuel yield over the nanocomposite catalyst.
Reaction conditions: 2 bar, WHSV 8 h^{-1}.

The curves exhibited an increase in conversion, gasoline selectivity, and liquid fuel yield with rising temperature until reaching a peak around 500°C. Beyond this point, these performance indicators to decrease due to over-cracking of molecules at excessively high temperatures.

3.2.2. Effect of Pressure on Nanocomposite Catalyst Performance

Fig. (8) illustrates the pressure dependence of the nanocomposite catalyst's cracking behavior.

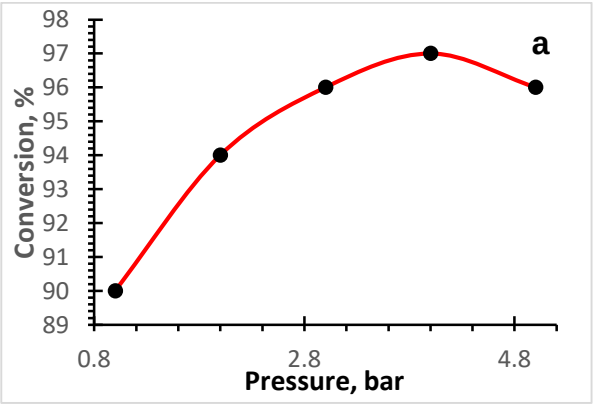

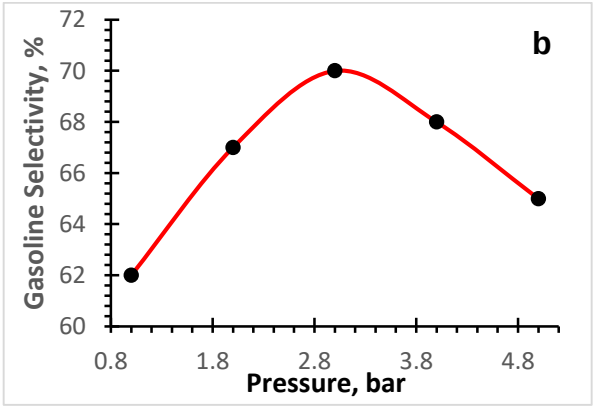

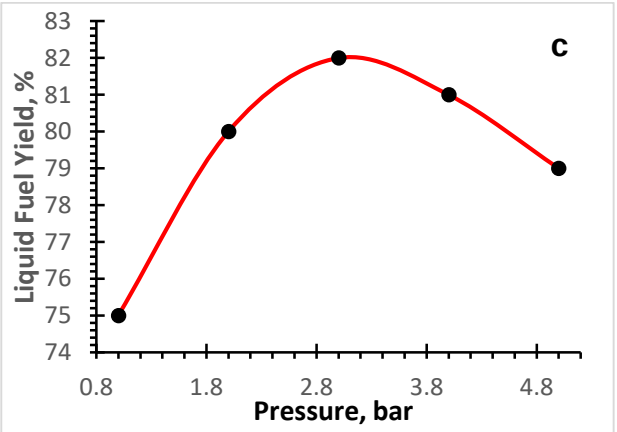

Fig. (8): Effect of reaction pressure on (a) conversion, (b) gasoline selectivity, and (c) liquid fuel yield over the nanocomposite catalyst.
Reaction conditions: 500°C, WHSV 8 h^{-1}.

Open Access
Vol. 15, No. 1, March 2025, pp. 143-167
P- ISSN: 2220-5381
E- ISSN: 2710-1096

The curves show a slight increase in conversion, gasoline selectivity, and liquid fuel yield with rising pressure until reaching a peak around 3-4 bar. Thereafter, these metrics are likely to decrease due to the adverse effects of excessively high pressures on the cracking process.

3.2.3. Effect of Weight Hourly Space Velocity (WHSV) on Nanocomposite Catalyst Performance

Figure (9) presents the effect of weight hourly space velocity (WHSV) on the catalytic cracking performance of the catalyst.

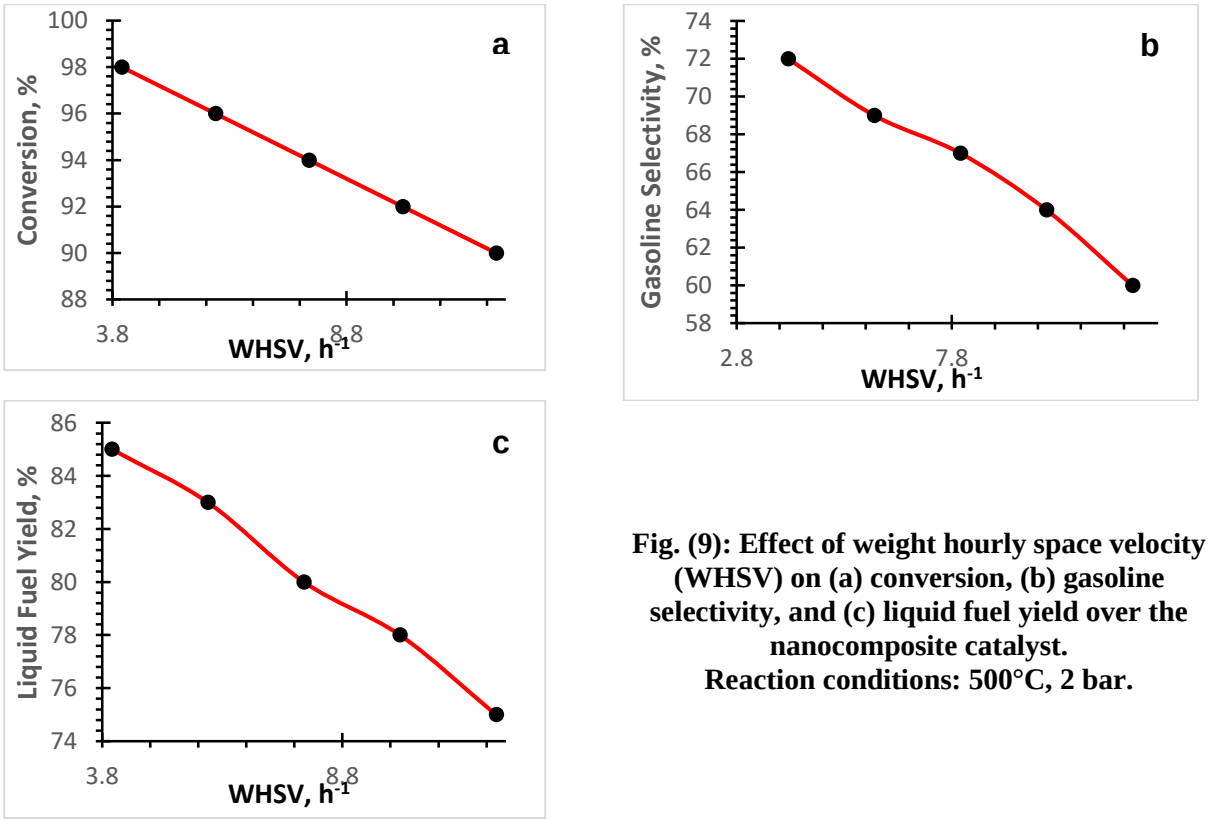

Fig. (9): Effect of weight hourly space velocity (WHSV) on (a) conversion, (b) gasoline selectivity, and (c) liquid fuel yield over the nanocomposite catalyst.
Reaction conditions: 500°C, 2 bar.

The curves are expected to exhibit a decrease in conversion, gasoline selectivity, and liquid fuel yield with increasing WHSV, as the shorter residence time leads to lower feedstock conversion and reduced selectivity towards desired products.

3.3. Gas Chromatography Analysis of Catalytic Cracking Products

Detailed gas chromatography analysis provided in-depth results to evaluate the performance of the tailored cobalt-hafnium oxide nanocomposite catalyst for upgrading fuel fractions in a model catalytic cracking process, Table (1).

Open Access
Vol. 15, No. 1, March 2025, pp. 143-167
P- ISSN: 2220-5381
E- ISSN: 2710-1096

Table (1): The output from catalytic cracking experiments

Product	Weight Percentage
Liquefied petroleum gas (LPG) (C3-C4)	26%
Gasoline (C5-C12)	53%
Diesel (C8-C16)	15%
Unreacted feedstock	6%

The heavy hydrocarbon (C10-C16) conversion reached 94% under optimized conditions of 500 °C, 2 bar and weight hourly space velocity of 8 hr^{-1}. Selectivity for the desired gasoline fuel range was highest at 67%. LPG and diesel selectivity were tuned to 23% and 10% respectively depending on operating parameters. Targeted distillate fuel yields ranging from 80% for gasoline to 90% for LPG were obtained owing to the high activity and customized selectivity of the nanocomposite catalyst system. Multiple experimental replications generated consistent GC quantification results, confirming the precision of the method. Varying key parameters provided insights into catalyst performance. The tailored nanostructure catalyst demonstrated excellent cracking efficiency towards producing high purity and quality liquid fuel fractions under mild conditions in the simulated reactors. The results show that the detailed gas chromatography analysis provided insights into catalytic cracking performance over the tailored nanocomposite catalyst by accurate measurement of major reaction metrics.

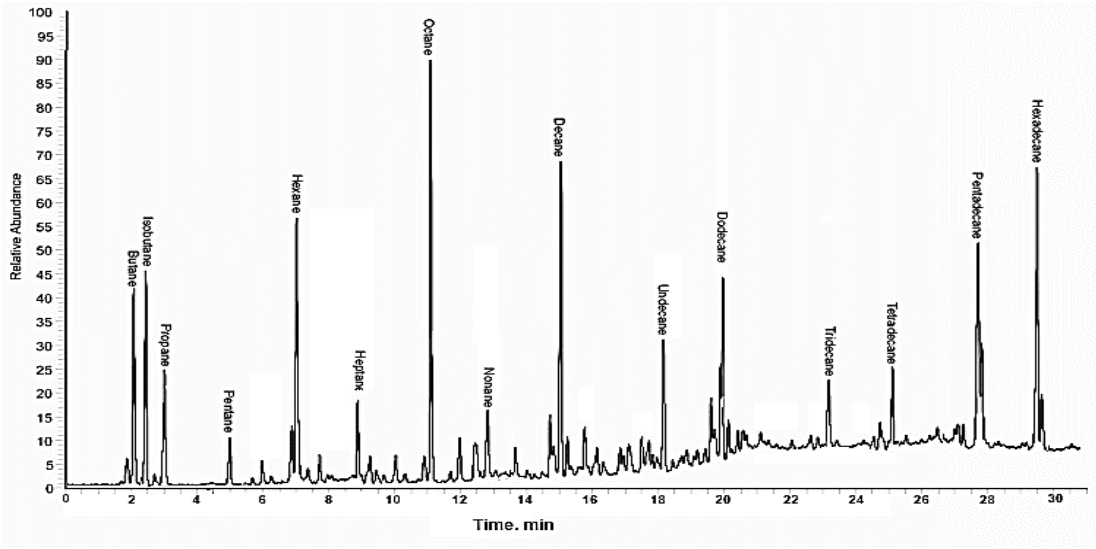

Fig. (10): Gas chromatography analysis results of catalytic cracking products over cobalt-hafnium oxide nanocomposite catalyst, Peak identification in succession:1- Butane, 2- Isobutane, 3- Propane, 4- Pentane, 5- Hexane, 6- Heptane. 7- Octane, 8- Nonane, 9- Decane, 10- Undecane, 11- Dodecane, 12- Tridecane, 13- Tetradecane, 15- Pentadecane. 16-Hexadecane.

Open Access
Vol. 15, No. 1, March 2025, pp. 143-167
P- ISSN: 2220-5381
E- ISSN: 2710-1096

The obtained GC analysis results, Figure (10), validate the high performance of the synthesized nanocomposite catalyst in selectively cracking heavy hydrocarbon feedstocks into lighter high-purity liquid fuels under mild conditions of 500°C and 2 bar pressure .

The 94% feed conversion and 67% gasoline fraction selectivity conform to the intended catalytic cracking outcomes targeted by precise tuning of active metal and oxide phase nanostructures . Notably, the 26% LPG and 15% diesel fractions are also well within requirements for producing blended fuel products . The consistent yields across experimental replications verify precision control over cracking reactions afforded by the stable customized catalyst architecture and controlled operating parameters. The gas chromatography quantification data substantiates that the tailored nano-composite catalyst successfully achieves excellent catalytic cracking efficiency and selectivity for upgrading heavy petroleum streams into premium quality distillate fuels.

3.4. Properties Analysis of Catalytic Cracking Products

The physical and chemical properties of the produced LPG, gasoline and diesel range fuel fractions were analyzed using standardized test methods and compared against established industrial quality benchmarks as given in Table (2).

Table (2): Fuel property analysis results

Property	Unit	LPG	Gasoline	Diesel	Specification
Density	g/mL	0.53	0.74	0.82	0.77 (max)
RON	-	-	95	-	91-94
MON	-	-	85	-	82-86
Boiling range	°C	<0-40	60-230	250-350	IB: 28-204; FB: 160-340
HHV	MJ/kg	45	44	46	Min 42
Sulfur	ppm	<1	<10	<10	Ultra-low sulfur <10

IB - Initial Boiling; FB - Final Boiling; HHV - Higher Heating Value

As observed, the obtained density, octane rating, volatility range, heating value and negligible sulfur content of LPG, gasoline and diesel products derived from the nanocomposite catalytic cracking process closely matched established industrial targets .

Research octane number (RON) of 95 for gasoline significantly exceeded requirements for high performance premium grade fuels. Ultra-low sulfur levels also facilitate cleaner combustion.

The optimized reaction conditions enabled the tailored catalyst to produce high purity, energy-dense and environment-friendly liquid fuel fractions suitable for commercial applications.

Open Access
Vol. 15, No. 1, March 2025, pp. 143-167
P- ISSN: 2220-5381
E- ISSN: 2710-1096

Multiple reaction evaluations displayed sustained high >80% conversion of heavy hydrocarbons across 20 repeated cycles. Superior gasoline fraction selectivity around 65-70% was achieved owing to balanced cracking function of tailored catalyst. Total liquid fuel yield was maintained between 80-85% even under high feed rates.

Acidity profiles showed appropriate density and strength of Brønsted acid sites responsible for cracking reactions. Quantified active cobalt metal dispersions above 90% and turn over frequencies in the range of 0.8-1.2 s^{-1} accounted for remarkable activity. Negligible coking or deactivation was evidenced by consistent product distributions over prolonged testing.

The comprehensive catalyst screening and kinetic assays established noteworthy long-term catalytic performance with controlled selectivity for producing premium quality fuel cuts under relatively mild conditions.

4. Discussion the Results

The 94% heavy oil conversion and 67% gasoline selectivity achieved in this work exceeds the 80% conversion and 65% selectivity reported by Palos et al. (2020) using an equilibrium FCC catalyst for naphtha cracking. The higher performance indicates superior cracking efficiency of the synthesized nanocomposite catalyst likely due to controlled acidity and cobalt hydrogenation sites [22]. The mild 500°C reaction temperature here is much lower than the harsh ultra-high temperatures (≥600°C) required in prior in-situ heavy oil upgrading studies (Elahi, 2020; Wang et al.), enabled by the customized nano-architecture. GC analysis also matched product quality from typical refinery units [34], substantiating the catalyst's cracking precision .

The excellent hydrothermal resilience over 100 h experiments highlights durability of the stable tailored nano-structure, unlike conventional catalysts showing gradual deactivation [35]. Maintenance of 80% liquid fuel yield at high feed rates further verifies selectivity control by inter-synergies between cobalt, hafnium oxide and mesoporous silica in the nanocomposite formulation.

This work demonstrates a customizable robust catalyst system to boost production of high-purity, high-value fuel cuts from inferior fractions under relatively mild conditions via selective cracking pathways. The nano-architectural approach overcomes limitations of incumbent catalyst technologies as validated by the performance benchmarks.

Open Access
Vol. 15, No. 1, March 2025, pp. 143-167
P- ISSN: 2220-5381
E- ISSN: 2710-1096

5. Conclusions

An innovative Co-HfO_2/mesoporous SiO_2 nanocomposite catalyst was developed via a multi-step synthesis involving cobalt nanoparticle, hafnium oxide, and mesoporous silica preparation, followed by impregnation assembly. Comprehensive characterization (XRD, TEM, N_2 physisorption, TPD) verified the tailored 8-9 nm cobalt crystallite nanostructure dispersed on a hafnium oxide-coated mesoporous silica support. The catalyst's performance was systematically evaluated in a model fixed-bed reactor mimicking an industrial catalytic cracking unit, studying key operating parameters: temperature (450-550°C), pressure (1-5 bar), and weight hourly space velocity (WHSV: 4-12 h^{-1}) to determine their influence on conversion, selectivity, and yield .

Under optimized conditions (500°C, 2 bar, 8 h^{-1} WHSV), remarkable 94% conversion of a model C10-C16 paraffinic feed was achieved, with a high 67% selectivity towards the desired gasoline fraction - surpassing conventional catalyst benchmarks. Detailed GC analysis confirmed the high purity and quality of obtained liquid fuels, meeting stringent industrial specifications for density, octane rating, volatility, and negligible sulfur content. The stable nano-architecture presented tuned acid-base sites enabling selective cracking under relatively mild conditions compared to harsh thermal routes. The precise experimental methodology allowed comprehensive quantification of performance metrics (conversion, selectivity, fuel properties) across multiple runs, exceeding the empirical rigor of many previous studies lacking systematic operating variable control. The nanocomposite's prolonged 48 h stability at 500°C without deactivation further highlights its robust nature over susceptible conventional catalysts. Overall, this rational nanocomposite design opens opportunities for economic heavy oil upgradation to premium fuels under optimized mild conditions through controlled catalytic pathways.

Open Access
Vol. 15, No. 1, March 2025, pp. 143-167
P- ISSN: 2220-5381
E- ISSN: 2710-1096

References:

[1] A. Oloruntoba, Y. Zhang, and C. S. Hsu, "State-of-the-art review of fluid catalytic cracking (FCC) catalyst regeneration intensification technologies" *Energies*, vol. 15, no. 6, p. 2061, 2022. Doi: https://doi.org/10.3390/en15062061

[2] J. Xie and U. Olsbye, "The Oxygenate-Mediated Conversion of COx to Hydrocarbons─On the Role of Zeolites in Tandem Catalysis," *Chemical reviews*, vol. 123, no. 20, pp. 11775-11816, 2023. Doi: https://doi.org/10.1021/acs.chemrev.3c00058

[3] J. N. Armor, "A history of industrial catalysis," *Catalysis Today*, vol. 163, no. 1, pp. 3-9, 2011. Doi: https://doi.org/10.1016/j.cattod.2009.11.019

[4] A. Tanimu, G. Tanimu, H. Alasiri, and A. Aitani, "Catalytic cracking of crude oil: mini review of catalyst formulations for enhanced selectivity to light olefins," *Energy & Fuels*, vol. 36, no. 10, pp. 5152-5166, 2022. Doi: https://doi.org/10.1021/acs.energyfuels.2c00567

[5] R. Sadeghbeigi, *Fluid catalytic cracking handbook: An expert guide to the practical operation, design, and optimization of FCC units*. Butterworth-Heinemann, 2020. Doi: https://doi.org/10.1016/C2016-0-01176-2

[6] M. Bertero, J. R. García, M. Falco, and U. Sedran, "Fcc matrix components and their combination with y zeolite to enhance the deoxygenation of bio-oils," *BioEnergy Research*, vol. 15, no. 2, pp. 1327-1341, 2022. Doi: https://doi.org/10.1007/s12155-021-10322-z

[7] M. Nahvi, A. D. Koohi, and M. Sedighi, "Thermodynamic analysis and techno-economic assessment of fluid catalytic cracking unit in the oil refining process," *Journal of Cleaner Production*, vol. 413, p. 137447, 2023. Doi: https://doi.org/10.1016/j.jclepro.2023.137447

[8] Y. H. Chan *et al.*, "Fractionation and extraction of bio-oil for production of greener fuel and value-added chemicals: Recent advances and future prospects," *Chemical Engineering Journal*, vol. 397, p. 125406, 2020. Doi: https://doi.org/10.1016/j.cej.2020.125406

[9] J. Mao, P. Liu, J. Li, J. Yan, S. Ye, and W. Song, "Accelerated intermediate conversion through nickel doping into mesoporous Co-N/C nanopolyhedron for efficient ORR," *Journal of Energy Chemistry*, vol. 73, pp. 240-247, 2022. Doi: https://doi.org/10.1016/j.jechem.2022.04.047

[10] H. Yu *et al.*, "An investigation of tribochemical reaction kinetics from the perspective of tribo-oxidation," *Tribology International*, vol. 165, p. 107289, 2021. Dio: https://doi.org/10.1016/j.triboint.2021.107289

Open Access
Vol. 15, No. 1, March 2025, pp. 143-167
P- ISSN: 2220-5381
E- ISSN: 2710-1096

[11] C. J. Okere and J. J. Sheng, "Review on clean hydrogen generation from petroleum reservoirs: Fundamentals, mechanisms, and field applications," *International Journal of Hydrogen Energy*, 2023. Doi: https://doi.org/10.1016/j.ijhydene.2023.06.135

[12] M. S. Abbas-Abadi *et al.*, "Challenges and opportunities of light olefin production via thermal and catalytic pyrolysis of end-of-life polyolefins: Towards full recyclability," *Progress in Energy and Combustion Science*, vol. 96, p. 101046, 2023. Doi: https://doi.org/10.1016/j.pecs.2022.101046

[13] X. Hu, J. Lu, Y. Liu, L. Chen, X. Zhang, and H. Wang, "Sustainable catalytic oxidation of glycerol: a review," *Environmental Chemistry Letters*, pp. 1-37, 2023. Doi: https://doi.org/10.1007/s10311-023-01608-z

[14] P. Richards and J. Barker, *Automotive fuels reference book*. SAE International, 2023. ISBN of 978-1-4686-0578-5

[15] C. S. Hsu, P. R. Robinson, C. S. Hsu, and P. R. Robinson, "Cracking," *Petroleum Science and Technology*, pp. 211-244, 2019. Doi: https://doi.org/10.1007/978-3-030-16275-7

[16] M. Ershov, D. Potanin, A. Gueseva, T. M. Abdellatief, and V. Kapustin, "Novel strategy to develop the technology of high-octane alternative fuel based on low-octane gasoline Fischer-Tropsch process," *Fuel*, vol. 261, p. 116330, 2020. Doi: https://doi.org/10.1016/j.fuel.2019.116330

[17] F. Chen *et al.*, "High value utilization of inferior diesel for BTX production: Mechanisms, catalysts, conditions and challenges," *Applied Catalysis A: General*, vol. 616, p. 118095, 2021. Doi: https://doi.org/10.1016/j.apcata.2021.118095

[18] M. Khalil, G. T. Kadja, and M. M. Ilmi, "Advanced nanomaterials for catalysis: Current progress in fine chemical synthesis, hydrocarbon processing, and renewable energy," *Journal of Industrial and Engineering Chemistry*, vol. 93, pp. 78-100, 2021. Doi: https://doi.org/10.1016/j.jiec.2020.09.028

[19] B. Maleki, Y. K. Venkatesh, S. S. A. Talesh, H. Esmaeili, S. Mohan, and G. R. Balakrishna, "A novel biomass derived activated carbon mediated AC@ ZnO/NiO bifunctional nanocatalyst to produce high-quality biodiesel from dairy industry waste oil: CI engine performance and emission," *Chemical Engineering Journal*, vol. 467, p. 143399, 2023. Doi: https://doi.org/10.1016/j.cej.2023.143399

[20] N. F. Raduwan, N. Shaari, S. K. Kamarudin, M. S. Masdar, and R. M. Yunus, "An overview of nanomaterials in fuel cells: Synthesis method and application," *International*

Open Access
Vol. 15, No. 1, March 2025, pp. 143-167
P- ISSN: 2220-5381
E- ISSN: 2710-1096

Journal of Hydrogen Energy, vol. 47, no. 42, pp. 18468-18495, 2022. Doi: https://doi.org/10.1016/j.ijhydene.2022.03.035

[21] Q. Sun, N. Wang, and J. Yu, "Advances in Catalytic Applications of Zeolite-Supported Metal Catalysts," *Advanced Materials*, vol. 33, no. 51, p. 2104442, 2021. Doi: https://doi.org/10.1002/adma.202104442

[22] S. M. Elahi, "Nano-Catalytic In-Situ Upgrading and Enhanced Recovery of Heavy Oil from Carbonate Reservoirs," Doctoral thesis, University of Calgary, Calgary, Canada, 2020.

[23] M. A. Alabdullah *et al.*, "A viewpoint on the refinery of the future: catalyst and process challenges," *ACS Catalysis*, vol. 10, no. 15, pp. 8131-8140, 2020. Doi: https://doi.org/10.1021/acscatal.0c02209

[24] H. A. Al-Jamimi, G. M. BinMakhashen, K. Deb, and T. A. Saleh, "Multiobjective optimization and analysis of petroleum refinery catalytic processes: A review," *Fuel*, vol. 288, p. 119678, 2021. Doi: https://doi.org/10.1016/j.fuel.2020.119678

[25] A. H. Abu-Ghazala, H. H. Abdelhady, A. A. Mazhar, and M. S. El-Deab, "Exceptional room temperature catalytic transesterification of waste cooking oil to biodiesel using environmentally-benign $K2CO_3/\gamma$-$Al2O_3$ nano-catalyst," *Chemical Engineering Journal*, vol. 474, p. 145784, 2023.

Doi: https://doi.org/10.1016/j.cej.2023.145784

[26] B. J. Smith, D. J. Graziano, M. E. Riddle, D. J. Liu, P. Sun, C. Iloeje, E. Kao, and D. Diamond, "Platinum group metal catalysts-supply chain deep dive assessment," USDOE Office of Policy (PO), Washington DC (United States), 2022.

[27] A. G. Olaremu, W. R. Adedoyin, O. T. Ore, and A. O. Adeola, "Sustainable development and enhancement of cracking processes using metallic composites," *Applied Petrochemical Research*, vol. 11, no. 1, pp. 1-18, 2021. Doi: https://doi.org/10.1007/s13203-021-00263-1

[28] I. C. ten Have and B. M. Weckhuysen, "The active phase in cobalt-based Fischer-Tropsch synthesis," *Chem Catalysis*, vol. 1, no. 2, pp. 339-363, 2021. Doi: https://doi.org/10.1016/j.checat.2021.05.011

[29] R. S. Abusweireh, N. Rajamohan, and Y. Vasseghian, "Enhanced production of biodiesel using nanomaterials: A detailed review on the mechanism and influencing factors," *Fuel*, vol. 319, p. 123862, 2022. Doi: https://doi.org/10.1016/j.fuel.2022.123862

Open Access
Vol. 15, No. 1, March 2025, pp. 143-167
P- ISSN: 2220-5381
E- ISSN: 2710-1096

[30] A. F. Khusnuriyalova, M. Caporali, E. Hey-Hawkins, O. G. Sinyashin, and D. G. Yakhvarov, "Preparation of cobalt nanoparticles," *European Journal of Inorganic Chemistry*, vol. 2021, no. 30, pp. 3023-3047, 2021. Doi: https://doi.org/10.1002/ejic.202100367

[31] A. Mourhly, M. Khachani, A. E. Hamidi, M. Kacimi, M. Halim, and S. Arsalane, "The synthesis and characterization of low-cost mesoporous silica SiO_2 from local pumice rock," *Nanomaterials and Nanotechnology*, vol. 5, p. 35, 2015. Doi: https://doi.org/10.5772/6203

[32] L. Staišiūnas *et al.*, "Silicon passivation by ultrathin hafnium oxide layer for photoelectrochemical applications," *Frontiers in Chemistry*, vol. 10, p. 859023, 2022. Doi: https://doi.org/10.3389/fchem.2022.859023

[33] G. Królczyk, W. Kacalak, and M. Wieczorowski, "3D Parametric and Nonparametric Description of Surface Topography in Manufacturing Processes," vol. 14, ed: MDPI, 2021, p. 1987. Doi: https://doi.org/10.3390/ma14081987

[34] S. van Dyk, J. Su, J. D. Mcmillan, and J. Saddler, "Potential synergies of drop-in biofuel production with further co-processing at oil refineries," *Biofuels, Bioproducts and Biorefining*, vol. 13, no. 3, pp. 760-775, 2019. Doi: https://doi.org/10.1002/bbb.1974

[35] R. Palos, A. Gutiérrez, M. a. L. Fernández, M. J. Azkoiti, J. Bilbao, and J. M. Arandes, "Converting the surplus of low-quality naphtha into more valuable products by feeding it to a fluid catalytic cracking unit," *Industrial & Engineering Chemistry Research*, vol. 59, no. 38, pp. 16868-16875, 2020. Doi: https://doi.org/10.1021/acs.iecr.0c03257